JOC Article

Stereoselective Stille Coupling of Enantiopure Haloallenes and Alkenylstannanes for the Synthesis of Allenyl Carotenoids. Experimental and Computational Studies

Belén Vaz, Raquel Pereira, Martín Pérez, Rosana Álvarez,* and Angel R. de Lera*

Departamento de Química Orgánica, Facultad de Química, Universidade de Vigo, 36310 Vigo, Spain

qolera@uvigo.es; rar@uvigo.es

Received April 8, 2008

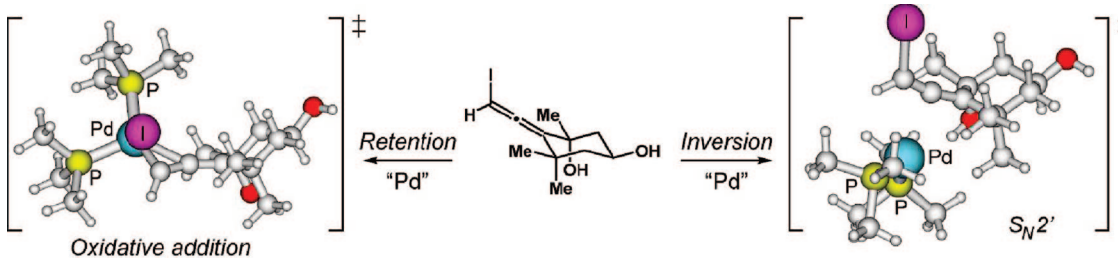

The stereoselectivity of the Stille cross-coupling of chiral enantiopure haloallenes and alkenylstannanes en route to allenic carotenoids is shown to depend on the nature of the halogen and palladium catalyst as well as on the presence of DMF as coordinating ligand and solvent. The results are consistent with DFT studies (B3LYP/6-31G*) on haloallene model systems, which compare the energetics of the competing oxidative addition to the allene−halogen bond (with retention of configuration) and the S_N2' displacement of the haloallene (with inversion of configuration) by the palladium complex.

Introduction

Carotenoids, an important family of chemically sensitive natural pigments isolated from plant and animal kingdoms, have been traditionally synthesized by C=C double bond forming strategies.[1] Classical condensations, prominently the Wittig and the Julia olefinations performed in consecutive fashion, have proven efficient for the preparation of carotenoids even at the industrial scale.[2] The generally more stereoselective transition-metal-catalyzed reactions[3] for C−C single bond formation have recently been applied to the preparation of both symmetrical and nonsymmetrical highly functionalized carotenoids.[4] The synthesis of peridinin **1**[5] (Figure 1),[6] a C37-norcarotenoid[7] with an abnormal arrangement of methyl groups on the side chain and endowed also with a γ-alkylidenebutenolide ring, five chiral centers, and the chiral allene axis, has been a *tour de force* in this regard. Two alternative synthetic approaches to peridinin featured the application of either convergent or sequential Stille cross-coupling reactions to construct the final polyene or the functionalized fragments from which the carotenoid was acquired with the application of a (Sylvestre) Julia olefination.[6a,b]

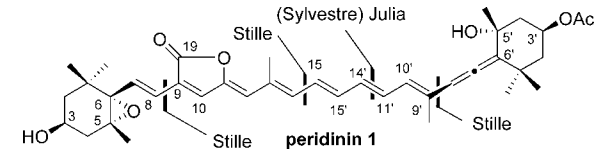

FIGURE 1. Synthetic approaches to peridinin **1** featuring Stille coupling reactions.

(1) For recent monographs, see: (a) Britton, G., Liaaen-Jensen, S., Pfander, H., Eds. *Carotenoids. Part 1A. Isolation and Analysis*; Birkhäuser: Basel, Switzerland, 1995. (b) Britton, G., Liaaen-Jensen, S., Pfander, H., Eds. *Carotenoids. Part 1B. Spectroscopy*; Birkhäuser: Basel, Switzerland, 1995.

(2) Britton, G., Liaaen-Jensen, S., Pfander, H. ,Eds. *Carotenoids. Part 2. Synthesis*; Birkhäuser: Basel, Switzerland, 1996.

(3) (a) *Metal-Catalyzed Cross-Coupling Reactions*; de Meijere, A., Diederich, F., Eds.; Wiley-VCH: Weinheim, Germany, 2004. (b) Nicolaou, K. C.; Bulger, P. G.; Sarlah, D. *Angew. Chem., Int. Ed.* **2005**, *44*, 4442.

(4) (a) Zeng, F.; Negishi, E. *Org. Lett.* **2001**, *3*, 719. (b) Vaz, B.; Álvarez, R.; de Lera, A. R. *J. Org. Chem.* **2002**, *67*, 5040.

(5) For the isolation of peridinin **1**, see: Song, P. S.; Koka, P.; Prezelin, B. B.; Haxo, F. T. *Biochemistry* **1976**, *15*, 4422.

(6) (a) Vaz, B.; Álvarez, R.; Brückner, R.; de Lera, A. R. *Org. Lett.* **2005**, *7*, 545. (b) Vaz, B.; Domínguez, M.; Álvarez, R.; de Lera, A. R. *Chem.—Eur. J.* **2007**, *13*, 1273. For other synthetic approaches to peridinin, see: (c) Furuichi, N.; Hara, H.; Osaki, T.; Mori, H.; Katsumura, S. *Angew. Chem., Int. Ed.* **2002**, *41*, 1023. (d) Furuichi, N.; Hara, H.; Osaki, T.; Nakano, M.; Mori, H.; Katsumura, S. *J. Org. Chem.* **2004**, *69*, 7949. (e) Olpp, T.; Brückner, R. *Angew. Chem., Int. Ed.* **2005**, *44*, 1553. (f) Olpp, T.; Brückner, R. *Angew. Chem., Int. Ed.* **2006**, *45*, 4023.

(7) For standard nomenclature and numbering of carotenoids, see: (a) IUPAC Commission on Nomenclature of Organic Chemistry and the IUPAC-IUB Commission on Biochemical Nomenclature. *Pure Appl. Chem.* **1975**, *41*, 407. (b) Weedon, B. C. L.; Moss, G. P. *Structure and Nomenclature*; in ref 1a, Chapter 3, p 27.

10.1021/jo800756b CCC: $40.75
Published on Web 08/06/2008

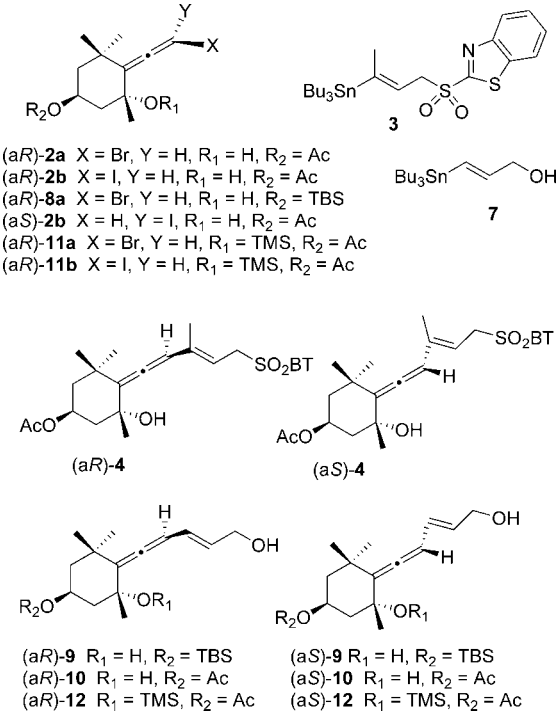

FIGURE 2. Reactants and vinyallene products resulting from the Stille coupling reactions (see Table 1).

In order to fully exploit the potential of the metal-catalyzed single bond forming processes in the synthesis of polyenes, the retention of configuration of the alkenyl coupling partners (halides or triflates as electrophiles, several metals as nucleophiles) must be obeyed.[3] Although this is often the case,[8] allene-containing polyenes add a further complication to the stereoselectivity analysis since both retention and inversion of configuration at the allene chiral axis[9] are possible when enantiopure allene partners are used in the coupling. During the peridinin synthetic endeavor,[6a] we observed that the Stille reaction of bromoallene (a*R*)-**2a** and stannane **3** (Figure 2) took place with inversion of configuration of the chiral axis to give (a*R*)-**4** (Table 1, entry 1) leading finally to the 6′-epimer of the natural product.[6a,b]

Vermeer et al. previously reported that enantiopure 1-bromoallenes reacted with the organozinc reagent Ph_2Zn using $Pd(PPh_3)_4$ as catalyst to afford the phenyl-substituted allenes with complete inversion of configuration, but 1-iodoallenes coupled with retention of configuration at the allene moiety under the same Negishi reaction conditions.[10] To our disappointment, our first Stille coupling trials using iodoallene (a*R*)-**2b** and stannane **3** provided a stereorandom mixture of the vinylallenes (a*S*)-**4** and (a*R*)-**4**, the products of inversion and retention of configuration, respectively.

Concerned with the inconsistencies on the stereochemical outcomes of Pd-catalyzed cross-coupling processes that differ on the organometallic component, we decided to carry out a comprehensive study of the stereoselectivity of the Stille coupling of enantiopure haloallenes **2** (X = I, Br) and related substrates with two different alkenylstannanes **3** and **7**. The main finding of this study is that the bias of substrate **2** to react with the palladium catalyst at the Csp^2 position vicinal to the axial tertiary hydroxyl group can be shifted to the direct oxidative addition reaction using a palladium catalyst that includes a coordinating solvent as ligand (DMF). Alternatively, protection of the hydroxyl group also hinders the S_N2' displacement of the allenyl halide. Computational studies of the competing metal-mediated processes are in agreement with the experimental findings and confirm the intriguing role played by the axial tertiary hydroxyl group of reactant **2**.

Results and Discussion

In the absence of precedents, except our previous results on the Stille cross-coupling reaction of chiral enantiopure haloallenes with alkenylstannanes,[6a,b] a survey of reaction conditions for the coupling between haloallenes **2**, **8**, **11**, and alkenylstannanes **3** and **7** was carried out. The most significant results from the series of reaction conditions and palladium sources surveyed are listed in Table 1.

The reaction of **3** with bromoallene (a*R*)-**2a** was highly diastereoselective (entries 1 and 2) and afforded sulfone (a*S*)-**4**, the product of inversion of configuration, as confirmed by X-ray diffraction analysis.[11] Inversion of configuration was also predominantly obtained using iodoallene (a*R*)-**2b** (entries 3−5), although allene (a*R*)-**4** was also produced in appreciable amounts (entries 4 and 5) when Pd_2dba_3 was used as catalyst at 25 °C. Bulky phosphines (entry 5) slowed down the reaction rates, and starting material was partially recovered. Thus, we did not observe the results reported by Vermeer for organozinc reagents showing a clear dependence of the diastereoselectivity on the nature of the halogen (Br: inversion; I: retention).

The inversion of configuration of the allene axis in both Stille and Negishi couplings could be the consequence of an initial *anti*-S_N2' displacement of halide by palladium.[12] In the case of (a*R*)-**2**, this transformation would generate **6**-*anti*, and this intermediate would undergo a suprafacial-[1,3]-sigmatropic shift of propargyl to allenyl palladium,[12c] leading to (a*S*)-**5** before transmetalation and progression through the catalytic cycle (Figure 3).[13] A more favored *anti*-S_N2' displacement, as opposed to the oxidative addition and the alternative *syn*-S_N2' reaction, would explain the configuration of the product (a*S*)-**4** (inversion) upon reaction of (a*R*)-**2a**. These pathways appear to be competi-

(8) (a) For examples of partial isomerization in Pd-catalyzed alkynylation with alkenyl halides, see: Shi, J.; Zeng, X.; Negishi, E. *Org. Lett.* **2003**, *5*, 1825. (b) For examples of clean inversion of configuration with organozinc reagents, see: Zeng, X.; Hu, Q.; Qian, M.; Negishi, E. *J. Am. Chem. Soc.* **2003**, *125*, 13636.

(9) (a) For recent review and monographs on allenes, see: KrauseN.; HashmiA. S. K. *Modern Allene Chemistry*; Wiley-VCH: Weinheim, Germany, 2004. (b) Ma, S. *Chem. Rev.* **2005**, *105*, 2829.

(10) (a) Ruitenberg, K.; Kleijn, H.; Elsevier, C. J.; Meijer, J.; Vermeer, P. *Tetrahedron Lett.* **1981**, *22*, 1451. (b) Elsevier, C. J.; Mooiweer, H. H.; Kleijn, H.; Vermeer, P. *Tetrahedron Lett.* **1984**, *25*, 5571. (c) Elsevier, C. J.; Vermeer, P. *J. Org. Chem.* **1985**, *50*, 3042. (d) Elsevier, C. J.; Kleijn, H.; Boersma, J.; Vermeer, P. *Organometallics* **1986**, *5*, 716.

(11) (a*S*)-**4** (CCDC-267166): Empirical formula ($C_{24}H_{29}NO_5S_2$). Formula weight (475.60). Temperature [173(2) K]. Wavelength (0.71073 Å). Crystal system (Monoclinic). Space group [*P*2(1)]. Unit cell dimensions (a = 10.2154(8) Å, α = 90°, b = 21.8191(17) Å, β = 106.447(2)°, c = 11.5734(9) Å, γ = 90°). Volume (2474.1(3) Å^3), *Z* (4). Density (calculated) (1.277 Mg/m^3). Absorption coefficient (0.249 mm^{-1}). *F*(000) [1008]. Crystal size (0.49 × 0.33 × 0.24 mm^3). Theta range for data collection (1.83 to 28.03°). Index ranges (−13 = h = 11,−24 = k = 28,−14 = l = 15). Reflections collected (15659). Independent reflections 9768 [R(int) = 0.0259]. Completeness to theta = 28.03° (96.6%). Absorption correction (SADABS). Max and min transmission (1.000000 and 0.874679). Refinement method (full-matrix least-squares on *F*2), Data/restraints/parameters (9768/1/594). Goodness-of-fit on *F*2 (0.862). Final R indices [I > 2σ(I)] (R1 = 0.0400, wR2 = 0.0652). R indices (all data) (R1 = 0.0600, wR2 = 0.0695). Absolute structure parameter [0.00(4)]. Largest diff. peak and hole (0.274 and −0.281 e•Å^{-3})

(12) For these mechanistic proposals, see: (a) Senn, H. M.; Ziegler, T. *Organometallics* **2004**, *23*, 2980. (b) Stille, J. K.; Lau, K. S.Y. *Acc. Chem. Res.* **1977**, *10*, 434. For palladium rearrangement, see: (c) Takahashi, Y.; Tsutsumi, K.; Nakagai, Y.; Morimoto, T.; Kakiuchi, K.; Ogoshi, S.; Kurosawa, H. *Organometallics* **2008**, *27*, 276.

TABLE 1. Diastereoselectivity on the Stille Coupling of Haloallenes 2, 8, and 11 and Stannanes 3 and 7 under Different Reaction Conditions

No.	haloallene	stannane	product	conditions[a–e]	solvent	*t* (h)	yield (%)[f]	(a*R*):(a*S*)[g]
1	(a*R*)-**2a**	**3**	**4**	a	DMF/THF	3	73	0:100
2	(a*R*)-**2a**	**3**	**4**	b	DMF	2	80	0:100
3	(a*R*)-**2b**	**3**	**4**	a	DMF	3.5	40	29:71
4	(a*R*)-**2b**	**3**	**4**	b	DMF	1	62	42:58
5	(a*R*)-**2b**	**3**	**4**	c	dioxane	6	40[h]	40:60[i]
6	(a*R*)-**8a**	**7**	**9**	b	DMF	1	63	*0:100*
7	(a*R*)-**8a**	**7**	**9**	a	DMF	3	84	*0:100*
8	(a*R*)-**8a**	**7**	**9**	d	DMF	20	52	40:60
9	(a*R*)-**8a**	**7**	**9**	e	DMF	8	88	32:68
10	(a*R*)-**2b**	**7**	**10**	b	DMF	1	89	28:72
11	(a*R*)-**2b**	**7**	**10**	a	DMF	3	89	42:58
12	(a*R*)-**2b**	**7**	**10**	d	DMF	20	51	*100:0*
13	(a*R*)-**2b**	**7**	**10**	e	DMF	2.5	63	*100:0*
14	(a*S*)-**2b**	**7**	**10**	b	DMF	1	89	14:86
15	(a*S*)-**2b**	**7**	**10**	a	DMF	3	95	40:60
16	(a*S*)-**2b**	**7**	**10**	d	DMF	20	51	0:100
17	(a*R*)-**11a**	**7**	**12**	e	DMF	15	92	100:0
18	(a*R*)-**11a**	**7**	**12**	b	DMF	1.5	98	79:21
19	(a*R*)-**11b**	**7**	**12**	e	DMF	3	39	100:0
20	(a*R*)-**11b**	**7**	**12**	b	DMF	1.5	60	90:10

[a] $PdCl_2(PhCN)_2$ (20%), *i*-Pr_2NEt. [b] $Pd_2dba_3 \cdot CHCl_3$ (10%). [c] Pd_2dba_3 (10%), DPPB (di-*tert*-butylbiphenylphosphine), $Ph_2PO_2NBu_4$. [d] Pd_2dba_3 (10%), $AsPh_3$. [e] $Pd(PPh_3)_4$ (10%). All reactions were performed at 25 °C. [f] Yields refer to the mixture of reaction products. [g] The ratio was determined by integration of ^1H NMR signals on the reaction mixtures (entries 1−5) or after isolation of the vinylallenes by chromatography (entries 6−20). [h] 75% conversion. [i] Taken from ref 6a.

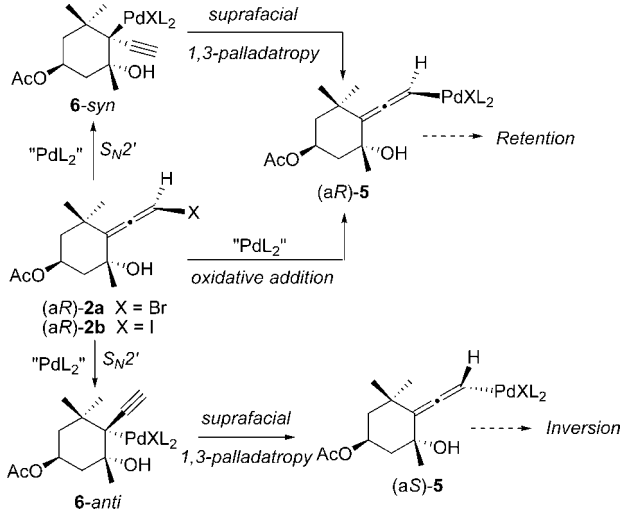

FIGURE 3. Oxidative addition or S_N2' displacement (*syn* and *anti*) by palladium on haloallenes determines the configuration of the product, as shown for substrate **2**.

tive for iodides (a*R*)-**2b** in accordance with the appearance of the retention product (a*R*)-**4**, which is presumably formed through allenyl palladium (a*R*)-**5** (Figure 3).

Stannane **7** also produced a single diastereomer (a*S*)-**9** from (a*R*)-**8a** upon treatment with $Pd_2dba_3 \cdot CHCl_3$ or $PdCl_2(PhCN)_2$ in the presence of *i*-Pr_2NEt as catalysts (entries 6 and 7), and thus these conditions favor the S_N2' reaction of allenylbromides. It has been reported that a coordinating solvent (such as DMF, NMP, or THF) generates a more reactive PdL(S) species in equilibrium with PdL_2 in palladium-catalyzed cross-coupling

SCHEME 1[a]

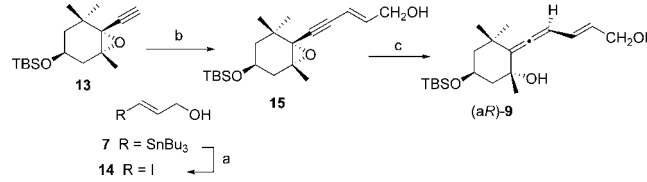

[a] Reagents and reaction conditions: (a) I_2, CH_2Cl_2, 25 °C (85%); (b) $Pd(PPh_3)_4$, CuI, (*i*-$Pr)_2NH$, 25 °C (84%); (c) DIBAL-H, CH_2Cl_2, 0 °C (50%).

reactions.[14] The possibility that palladium complexes containing PdL_2 or PdL(DMF) (L = $AsPh_3$ or PPh_3) also promote a faster oxidative addition to (a*R*)-**8a** was tested. In fact, the use of these conditions with (a*R*)-**8a** led to mixtures of retention and inversion vinylallene products (a*R*)-**9**/(a*S*)-**9** [$Pd(AsPh_3)_4$, entry 8, 40:60; $Pd(PPh_3)_4$, entry 9, 32:68], although longer reaction times were needed. Interestingly, these modifications altered the stereochemical course of the coupling of iodoallenes, affording the retention product (a*R*)-**10** as the only edduct from the coupling of iodide (a*R*)-**2b** and stannane **7** (entries 12 and 13). Evidence for the stereochemical outcome was obtained for (a*S*)-**4** by X-ray analysis as described[6] and for (a*R*)-**9** by comparison of the ^1H NMR spectra[15a] with those of the vinylallene obtained alternatively with retention of configuration using the well-defined stereospecific *syn*-S_N2' reduction of alkynyloxiranes with excess DIBAL-H (Scheme 1).[15b]

In order to examine a potential coordination effect of the hydroxyl group, which would contribute to favor the S_N2' displacement at the proximal Csp^2-allene atom, we carried out the coupling of **7** with epimer iodoallene (a*S*)-**2b** and also with allenes (a*R*)-**11a** and (a*R*)-**11b** having a TMS-protected hydroxyl group (Table 1). In all cases, the main (entries 14, 15, 18, and 20) or exclusive product (entries 16, 17, and 19) showed retention of configuration with the different sources of palladium

(13) Other isomerization mechanism cannot be discarded. Allenyl palladium intermediates have been proposed to isomerize in the presence of monodentate palladium ligands: Yoshida, M.; Hayashi, M.; Shishido, K. *Org. Lett.* **2007**, *9*, 1643. In addition, optically active allenylpalladium species are racemized through the formation of dinuclear complexes: Ogoshi, S.; Nishida, T.; Shinagawa, T.; Kurosawa, H. *J. Am. Chem. Soc.* **2001**, *123*, 7164. Moreover, allenes are configurationally unstable in the presence of Pd(II)/LiBr through *anti*-bromopalladation processes: Horváth, A.; Bäckvall, J. E. *Chem. Commun* **2004**, 964.

(14) (a) Amatore, C.; Bacaille, A.; Fuxa, A.; Jutand, A.; Meyer, G.; Ndedi Ntepe, A. *Chem.—Eur. J.* **2001**, *7*, 2134. (b) Amatore, C.; Bahsoun, A. A.; Jutand, A.; Meyer, G.; Ndedi Ntepe, A.; Ricard, L. *J. Am. Chem. Soc.* **2003**, *125*, 4212. (c) Ahlquist, M.; Norrby, P.-O. *Organometallics* **2007**, *26*, 550.

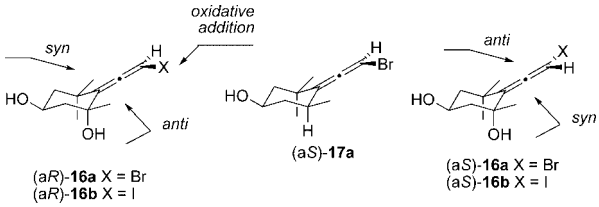

FIGURE 4. Haloallene model systems used in the computational study of the competing *syn*-S_N2' and *anti*-S_N2' displacements and the oxidative addition reaction with $Pd(PMe_3)_2$ and $Pd(PMe_3)$(DMF) as palladium catalysts.

regardless of the halogen used. The protected bromoallene (a*R*)-**11a** produced efficiently (92% yield) the corresponding vinylallene (a*R*)-**12** with retention of configuration. Thus, it appears that the proximal tertiary hydroxyl diverts the Stille reaction toward the formation of the undesired S_N2' product, and this effect could be counteracted with its protection as silyl ether.

Aimed to shed some light into the dependence of the diastereoselectivity with both the halogen and the palladium catalyst composition, we carried out a computational study of the competing processes, the oxidative addition into the Csp^2-Hal bond, and the S_N2' displacement of halogen by palladium with *anti* and *syn* trajectories. The model systems selected (Figure 4) were both axial diastereomers of the (deacetylated) haloallene **16** as well as the analogous bromoallene **17a** lacking the tertiary hydroxyl group (note the change of stereochemical descriptor of **17a** relative to **16** for the same relative arrangement of groups on the allene axis). Model palladium catalysts [$Pd(PMe_3)_2$] and [$Pd(PMe_3)$(DMF)] were reasonably chosen with a PMe_3 ligand that is smaller than PPh_3 and the same coordinating solvent used in the experiments.

The B3LYP/6-31G*-SDD computational level was used due to the satisfactory results obtained in previous computational studies for the Stille reaction to afford dienes.[16] All the calculations were performed with the Gaussian03 suite of programs.[17] The solvent effect (DMF) was taken into account with sequential single-point calculations at the gas-phase optimized geometries using a continuum model.[18] Figure 4 depicts the model systems and reactions used in the calculations, and Table 2 summarizes the energy values for the located transition structures of the selected transformations.

TABLE 2. Thermodynamic Data (Relative Free Energies of Activation $\Delta G^{\#}$, kcal/mol) of the Transition Strucures for the Model Reactions Depicted on Figure 4

			gas phase ($\Delta G^{\#}$)[a]			COSMO (DMF, $\Delta G^{\#}$)[b]		
entry	allene	catalyst	syn	anti	O.A.[b]	syn	anti	O.A.[c]
1	(a*R*)-**16a**	$Pd(PMe_3)_2$	24.9	*15.1*	20.1	30.7	22.6	*17.3*
2		$Pd(PMe_3)$(DMF)	20.4	*8.9*	8.1[d]	26.3	16.4	*9.2*[d]
3	(a*R*)-**16b**	$Pd(PMe_3)_2$	27.3	*16.9*	20.1	32.6	24.5	*18.7*
4		$Pd(PMe_3)$(DMF)	22.9	10.6	*7.4*[d]	27.9	17.9	*8.7*[d]
5	(a*S*)-**17a**	$Pd(PMe_3)_2$	25.9	20.4	*18.7*	31.2	24.5	*15.1*
6	(a*S*)-**16a**	$Pd(PMe_3)_2$	21.3	19.7	*14.9*	28.6	25.7	*13.3*
7	(a*S*)-**16b**	$Pd(PMe_3)_2$	22.3	21.1	*13.8*	29.8	26.9	*14.1*

[a] Gas phase. [b] DMF (COSMO). [c] Oxidative addition. [d] $\Delta G^{\#}$ for the oxidative addition to the monophosphine complex $Pd(PMe_3)$ obtained formally from the dissociation of DMF from the starting $Pd(PMe_3)$(DMF).

The two main findings of the computations are the effect of the catalyst composition, in particular, the presence of a coordinating solvent as palladium ligand, and the role of the tertiary hydroxyl group of the substrates.

First, when computing the oxidative addition reaction of (a*R*)-**16a** and (a*R*)-**16b** with $Pd(PMe_3)_2$ and $Pd(PMe_3)$(DMF) complexes, it was noted that the concerted transition structure for the latter model catalyst could not be located. Instead, we could characterize a stepwise process involving the loss of DMF followed by the oxidative addition via the monophosphine palladium complex.[19] This step shows energies of activation of 8.1 and 7.4 kcal/mol for (a*R*)-**16a** and (a*R*)-**16b**, respectively, which is consistent with previous reports of rate acceleration on the oxidative addition to aryl halides of monophosphine palladium complexes and also with the observation that highly bulky phosphines accelerate cross-coupling processes most likely entering the catalytic cycles as $Pd(PR_3)$ complexes.[20]

Regardless of the halogen, the lowest barrier computed for the reaction of (a*R*)-**16a** and (a*R*)-**16b** with $Pd(PMe_3)_2$ corresponds to the *anti*-S_N2' displacement (15.1 and 16.9 kcal/mol, respectively), in full agreement with our earlier findings. In contrast, the global barrier for the two-step oxidative addition of $Pd(PMe_3)$(DMF) to bromoallene (a*R*)-**16a** is similar to that of the *anti*-S_N2' competing reaction, which explains the stereorandom outcome experimentally obtained with (a*R*)-**8a** (Table 1, entries 8 and 9). Interestingly, the oxidative addition to iodoallene (a*R*)-**16b** is the most favored path when the mixed complex $Pd(PMe_3)$(DMF) is used (7.4 vs 10.6 kcal/mol for the oxidative addition and *anti*-S_N2', and 22.9 kcal/mol for the *syn*-S_N2'), in full agreement with the complete stereoselectivity of (a*R*)-**2b** and (a*S*)-**2b** obtained experimentally (Table 1, entries 12 and 16). Our computations confirm that the combined effect of the greater reactivity of the C−I bond and the more reactive palladium source [PdL(S)] contribute to the retention of configuration of the allenyl iodides through a "classical" Stille catalytic cycle starting from the concerted oxidative addition step.

The second observation from these studies is the effect on the S_N2' substitution reaction of the tertiary hydroxyl group located vicinal to the allene. Comparison of the energy values between pairs of epimers of **16a** and **16b** indicates that the axial hydroxyl group lowers the activation energy for the *anti*-S_N2' displacement in (a*R*)-**16** by about 5 kcal/mol. In fact, bromoal-

(15) (a) The resonance of the allene proton on the a*S* diastereomers is shifted downfield relative to those of the aR counterparts. (b) The preparation of carotenoid allenols from alkynyloxiranes was first described by Widmer, E. *Pure Appl. Chem.* **1985**, *57*, 741.

(16) (a) Álvarez, R.; Nieto Faza, O.; Silva López, C.; de Lera, A. R. *Org. Lett.* **2006**, *8*, 35. (b) Álvarez, R.; Nieto Faza, O.; de Lera, A. R.; Cárdenas, D. *Adv. Synth. Catal.* **2007**, *349*, 887. (c) Álvarez, R.; Pérez, M.; Nieto-Faza, O.; de Lera, A. R. *Organometallics* **2008**, in press. (d) For computational details see Supporting Information.

(17) Frisch, M. J. ; Trucks, G. W.; Schlegel, H. B.; Scuseria, G. E.; Robb, M. A.; Cheeseman, J. R.; MontgomeryJ. A., Jr.; Vreven, T.; Kudin, K. N. ; Burant, J. C.; Millam, J. M.; Iyengar, S. S.; Tomasi, J.; Barone, V.; Mennucci, B.; Cossi, M.; Scalmani, G.; Rega, N.; Petersson, G. A.; Nakatsuji, H.; Hada, M.; Ehara, M.; Toyota, K.; Fukuda, R.; Hasegawa, J.; Ishida, M.; Nakajima, T.; Honda, Y. ; Kitao, O.; Nakai, H.; Klene, M.; Li, X.; Knox, J. E.; Hratchian, H. P.; Cross, J. B.; Bakken, V.; Adamo, C.; Jaramillo, J.; Gomperts, R.; Stratmann, R. E.; Yazyev,O. ; Austin, A. J. ; Cammi, R. ; Pomelli, C. ; Ochterski, J. W. ; Ayala, P. Y. ; Morokuma, K.; Voth, G. A.; Salvador, P.; Dannenberg, J. J.; Zakrzewski, V. G.; Dapprich, S.; Daniels, A. D.; Strain, M. C.; Farkas, O.; Malick, D. K.; Rabuck, A. D.; Raghavachari, K.; Foresman, J. B.; Ortiz, J. V.; Cui, Q.; Baboul, A. G.; Clifford, S.; Cioslowski, J.; Stefanov, B. B.; Liu, G.; Liashenko, A.; Piskorz, P.; Komaromi, I.; Martin, R. L.; Fox, D. J.; Keith, T.; Al-Laham, M. A.; Peng, C. Y.; Nanayakkara, A.; Challacombe, M.; Gill, P. M. W.; Johnson, B.; Chen, W.; Wong, M. W.; Gonzalez, C.; Pople, J. A. *Gaussian03*; Gaussian, Inc.: Wallingford CT, 2004.

(18) (a) Onsager, L. *J. Am. Chem. Soc.* **1936**, *58*, 1486. (b) Tomasi, J.; Persico, M. *Chem. Rev.* **1994**, *94*, 2027. (c) Tomasi, J.; Mennucci, B.; Cammi, R. *Chem. Rev.* **2005**, *105*, 2999.

(19) Christmann, U.; Vilar, R. *Angew. Chem., Int. Ed.* **2005**, *44*, 366.

(20) (a) Goossen, L. J.; Koley, D.; Hermann, H. L.; Thiel, W. *Organometallics* **2006**, *25*, 54. (b) Ahlquist, M.; Fristrup, P.; Tanner, D.; Norrby, P. O. *Organometallics* **2006**, *25*, 2066. (c) Lam, K. C.; Marder, T. B.; Lin, Z. *Organometallics* **2007**, *26*, 758.

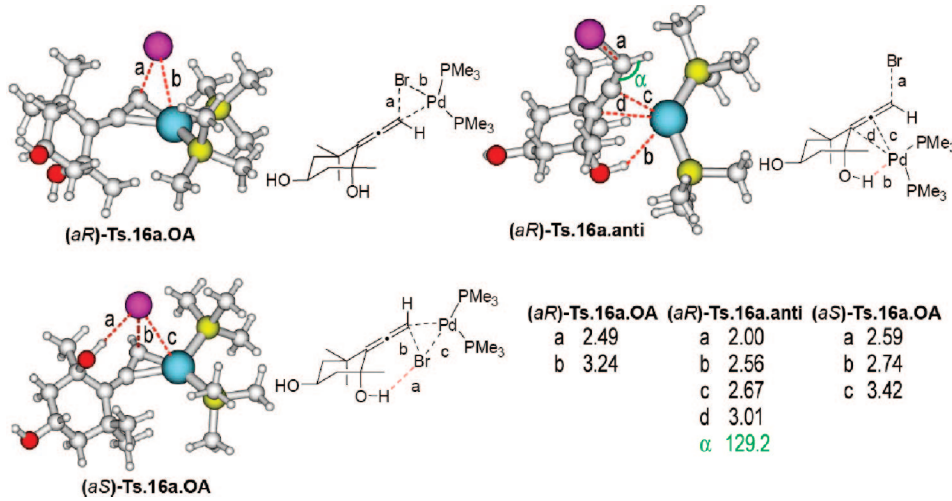

FIGURE 5. Transition structures (a*R*)-**TS.16a.OA**, (a*R*)-**TS.16a.anti**, and (a*S*)-**TS.16a.OA** for the oxidative addition (OA) and *anti*-S_N2' displacement of substrate **16a** with $Pd(PMe_3)_2$. Relevant bond distances (in angstroms) and bond angle (α, in degrees) are highlighted.

lene (a*S*)-**17a**, which lacks the hydroxyl, is predicted to couple with retention of configuration given the lowest energy computed for the oxidative addition reaction relative to the S_N2' alternative (18.7 vs 20.4 kcal/mol, Table 2, entry 5). Moreover, the axially oriented hydroxyl group appears to conversely increase the energy of activation of the competing oxidative addition process in these isomers (a*R*)-**16** by the same amount when compared to diastereomers (a*S*)-**16** (cf. Table 2, entries 1 and 6).

A potential role of the hydroxyl group in assisting the reaction is suggested by its distance to the palladium center in the transition state for the *anti*-S_N2' displacement [H−Pd bond distance of 2.56 Å for (a*R*)-**16a** and 2.57 Å for (a*R*)-**16b**, Figure 5]. Interactions between hydrogen bound to oxygen or nitrogen and transition metals in low oxidation states have been observed[21] and exhibit features of the classical hydrogen bond. A similar interaction between the hydroxyl and the halogen atoms as gathered from the elongated C−Br bond (2.74 vs 2.49 Å for (a*S*)-**16a** and (a*R*)-**16a**, respectively, Figure 5) might also explain the lower barriers obtained for the oxidative addition of (a*S*)-**16b** and (a*S*)-**16b** (14.9 and 13.8 kcal/mol, respectively).

Solvent effects were calculated using COSMO. In general, there is a lowering of the energies of activation for the oxidative addition processes most likely due to the concerted nature of the transition state. However, the reverse trend is computed for the halogen displacement processes (*syn* or *anti*, most pronounced for the latter). This is consistent with the polar nature of the S_N2' reaction, a process of associative/dissociative nature, which is not properly described by the current methods.

In summary, the Stille reaction of highly functionalized allenyl halides and alkenyl stannanes takes place with either retention (via oxidative addition) or inversion of configuration (via S_N2' displacement and 1,3-palladotropy) at the allene axis.[22] Both the nature of the halogen and the reaction conditions, particularly the free axial hydroxyl substituent and the presence of coordinating solvents as part of the composition of the palladium catalyst, play a crucial role on the stereochemical outcome. DFT computations of the competing reactivities of model systems, including an explicit solvent molecule on Pd, are consistent with the experimental results. Furthermore, the computations confirm the role of the hydroxyl group on further modulating the reactivity by providing assistance and/or stabilization of the reactive intermediates. Together these results are of value since they overcome the synthetic limitation previously reported during the Stille approach to allenic carotenoids.[6]

Experimental Section

(1*S*,3*R*,4a*R*)-3-Hydroxy-3,5,5-trimethyl-4-(2-iodovinylidene)cyclohexyl Acetate (a*R*)-2b. CuI (0.478 g, 2.51 mmol), NH_4I (0.182 g, 1.25 mmol), and HI (57% aq, 0.60 mL, 4.01 mmol) were added sequentially to a cooled (−10 °C) solution of (1*R*,3*S*,6*R*)-6-ethynyl-1,5,5-trimethyl-7-oxabicyclo[4.1.0]heptan-3-ol[6b] (0.457 g, 2.51 mmol) in Et_2O (11.0 mL). After stirring for 1.5 h, an aqueous solution of NH_4Cl/NH_3 1:1 (10 mL) was added, and the layers were separated. The organic layer was washed with brine (3×) and dried (Na_2SO_4), and the solvent was evaporated. The residue was purified by column chromatography (silica gel, 60:40 hexane/EtOAc) to afford 0.630 g (81%) of a white solid, which was used in the next step without further purification. Ac_2O (0.863 mL, 9.22 mmol) was added to a solution of the diol obtained before (0.568 g, 1.84 mmol) in pyridine (5.7 mL). After stirring for 3 h, the mixture was extracted with Et_2O (3×). The combined organic layers were washed with a saturated aqueous $CuSO_4$ solution (2×) and dried (Na_2SO_4), and the solvent was evaporated. The residue was purified by column chromatography (silica gel, gradient from 90:10 to 80:20 hexane/EtOAc) to afford 0.59 g (91%) of a white solid identified as (1*S*,3*R*,4a*R*)-3-hydroxy-3,5,5-trimethyl-4-(2-iodovinylidene)cyclohexyl acetate (a*R*)-**2b** and 0.05 g (8%) of a white solid identified as (1*S*,3*R*,4a*S*)-3-hydroxy-3,5,5-trimethyl-4-(2-iodovinylidene)cyclohexyl acetate (a*S*)-**2b**.

Data for (1*S*,3*R*,4a*R*)-**2b**: ^1H NMR (400 MHz, $CDCl_3$) δ 5.72 (s, 1H), 5.25 (m, 1H), 2.17 (ddd, J = 12.9, 4.1, 2.1 Hz, 1H), 1.97

(21) Hallman, K.; Frölander, A.; Wondimagegn, T.; Svensson, M.; Moberg, C. *Proc. Natl. Acad. Sci. U.S.A.* **2004**, *101*, 5400, and references cited therein.

(22) Unfortunately, we could not generalize this finding, due to the instability of the samples obtained when simple enantiopure iodoallenes **18** and **19** were coupled with alkenylstannane **7** under the optimized conditions.These enantiopure allenes were prepared using the S_N2' displacement of a propargylic mesylate with a cuprate, as described by Vermeer (Elsevier, C. J.; Meijer, J.; Tadema, G.; Stehouwer, P. M.; Bos, H. J. T.; Vermeer, P.; Runge, W. *J. Org. Chem.* **1982**, *47*, 2194−2196) and Marshall (Marshall, J. A.; Grant, C. M. *J. Org. Chem.* **1999**, *64*, 8214, respectively.

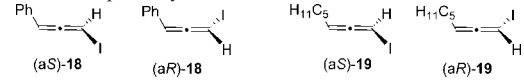

The copper-catalyzed N-allenylation of amides (Trost, B. M.; Stiles, D. T. *Org. Lett.* **2005**, *7*, 2117) using simple enantiopure iodoallenes takes place with retention of configuration (Shen, L.; Hsung, R. P.; Zhang, Y.; Antoline, J. E.; Zhang, X. *Org. Lett.* **2005**, *7*, 3081).

(s, 3H), 1.87 (dd, J = 12.4, 4.0, 2.1 Hz, 1H), 1.44 (t, J = 11.5 Hz, 2H), 1.4−1.3 (m, 1H), 1.36 (s, 3H), 1.30 (s, 3H), 1.10 (s, 3H) ppm; ^{13}C NMR (100 MHz, $CDCl_3$) δ 201.6 (s), 170.4 (s), 119.0 (s), 71.5 (s), 67.5 (d), 44.5 (t, 2×), 38.3 (d), 35.0 (s), 30.8 (q), 30.4 (q), 29.4 (q), 21.2 (q); MS (ESI$^+$) m/z (%) 374 (14), 373 (M^+ + 23, 100), 273 (11); HMRS (ESI$^+$) calcd for $C_{13}H_{19}INaO_3$, 373.0271; found, 373.0264. Anal. Calcd for $C_{13}H_{19}IO_3$: C, 44.59; H, 5.47. Found: C, 44.62; H, 5.44.

Data for (1*S*,3*R*,4a*S*)-**2b**: ^{1}H NMR (400 MHz, $CDCl_3$) δ 5.84 (s, 1H), 5.28 (m, 1H), 2.19 (ddd, J = 12.9, 4.2, 2.2 Hz, 1H), 1.98 (s, 3H), 1.89 (ddd, J = 12.3, 4.1, 2.2 Hz, 1H), 1.4−1.3 (m, 2H), 1.37 (s, 3H), 1.32 (s, 3H), 1.08 (s, 3H) ppm; ^{13}C NMR (100 MHz, $CDCl_3$) δ 200.7 (s), 170.2 (s), 118.9 (s), 71.2 (s), 67.5 (d), 44.7 (t), 44.5 (t), 38.7 (d), 34.7 (s), 31.9 (q), 30.6 (q), 28.1 (q), 21.2 (q); MS (ESI$^+$) m/z (%) 374 (13), 373 (M^+ + 23, 100), 273 (6); HMRS (ESI$^+$) calcd for $C_{13}H_{19}INaO_3$, 373.0271; found, 373.0263.

(−)-(1*R*,3*S*,6a*R*)-6-(2-Bromovinylidene)-3-(*tert*-butyldimethylsilyloxy)-1,5,5-trimethylcyclohexan-1-ol (a*R*)-8a. CuBr (0.23 g, 1.58 mmol), NH_4Br (0.08 g, 0.79 mmol), and HBr (48% aq, 0.29 mL, 2.53 mmol) were added sequentially to a cooled (−10 °C) solution of *tert*-butyldimethylsilyl (1*R*,3*S*,6*R*)-6-ethynyl-1,5,5-trimethyl-7-oxabicyclo[4.1.0]heptan-3-yl ether[6b] (0.47 g, 1.58 mmol) in Et_2O (7.7 mL). After stirring for 30 min, an aqueous solution of NH_4Cl/NH_3 1:1 (10 mL) was added, and the layers were separated. The organic layer was washed with brine (3×) and dried (Na_2SO_4), and the solvent was evaporated. The residue was purified by column chromatography (silica gel, gradient from 95:5 to 90:10 hexane/EtOAc) to afford 0.172 g (29%) of a white solid identified as (1*R*,3*S*,6a*R*)-6-(2-bromovinylidene)-3-(*tert*-butyldimethylsilyloxy)-1,5,5-trimethylcyclohexan-1-ol (a*R*)-**8a**. A fraction containing a mixture of products was further purified by HPLC (Nova-Pak HR, 6 mm, 30 × 1.9 cm, 97:3 hexane/AcOEt, 3 mL/min) to afford 8.1 mg of the corresponding (1*R*,3*S*,6a*S*)-6-(2-bromovinylidene)-3-(*tert*-butyldimethylsilyloxy)-1,5,5-trimethylcyclohexan-1-ol (a*S*)-**8a**.

Data for (a*R*)-**8a**: ^{1}H NMR (400 MHz, $CDCl_3$) δ 5.92 (s, 1H), 4.21 (m, 1H), 2.06 (ddd, J = 13.3, 4.2, 2.3 Hz, 1H), 1.74 (ddd, J = 12.8, 4.1, 2.3 Hz, 1H), 1.42 (dd, J = 13.3, 10.9 Hz, 1H), 1.37 (s, 3H), 1.4−1.3 (m, 1H), 1.27 (s, 3H), 1.09 (s, 3H), 0.88 (s, 9H), 0.06 (s, 6H) ppm; ^{13}C NMR (100 MHz, $CDCl_3$) δ 198.2 (s), 124.4 (s), 73.9 (d), 72.2 (s), 64.3 (d), 49.0 (t), 48.6 (t), 35.7 (s), 31.2 (q), 30.5 (q), 29.2 (q), 25.7 (q), 18.0 (s), −4.7 (q, 2×) ppm; MS (EI$^+$) m/z (%) 319 (M^+ − *t*Bu, 2), 317 (M^+ − *t*Bu, 2), 261 (19), 181 (100), 165 (91), 163 (21), 145 (38), 143 (17), 129 (20), 121 (33), 120 (16), 119 (21), 115 (28), 107 (28), 105 (70), 93 (44), 91 (24), 77 (16), 75 (97), 73 (58); HMRS (EI$^+$) calcd for $C_{13}H_{22}{}^{79}BrO_2Si$ [M^+ − *t*Bu], 317.0572; found, 317.0577; IR (NaCl) ν 3600−3100 (br, OH), 2958 (s, C−H), 2929 (s, C−H), 2857 (m, C−H), 1950 (w, C═C═C), 1470 (m), 1380 (m), 1256 (m, C−O), 1082 (s) cm^{-1}. Anal. Calcd for $C_{17}H_{31}BrO_2Si$: C, 54.39; H, 8.32. Found: C, 54.34; H, 8.37. $[\alpha]^{22}_D$ −30.9 (*c* 0.04, $CHCl_3$).

Data for (a*S*)-**8a**: ^{1}H NMR (400 MHz, $CDCl_3$) δ 6.10 (s, 1H), 4.23 (m, 1H), 2.07 (ddd, J = 13.1, 3.9, 2.2 Hz, 1H), 1.74 (ddd, J = 12.7, 4.1, 2.2 Hz, 1H), 1.36 (s, 2H), 1.3−1.2 (m, 3H), 1.31 (s, 3H), 1.07 (s, 3H), 0.86 (s, 9H), 0.06 (s, 6H) ppm; ^{13}C NMR (100 MHz, $CDCl_3$) δ 197.4 (s), 124.5 (s), 75.0 (d), 72.1 (s), 64.5 (d), 49.2 (t), 48.6 (t), 35.5 (s), 31.8 (q), 30.9 (q), 29.1 (q), 25.9 (q), 18.2 (s), −4.6 (q, 2×) ppm; MS (EI$^+$) m/z (%) 376 (M^+, 2), 374 (M^+, 2), 295 (12), 263 (29), 261 (32), 260 (19), 181 (11), 145 (12), 105 (12), 75 (100), 73 (50); HMRS (EI$^+$) calcd for $C_{17}H_{31}{}^{79}BrO_2Si$ [M^+], 374.1277; found, 374.1279; IR (NaCl) ν 3600−3100 (br, OH), 2958 (s, C−H), 2929 (s, C−H), 2856 (m, C−H), 1945 (w, C═C═C), 1472 (m), 1384 (m), 1256 (m, C−O), 1081 (s) cm^{-1}; $[\alpha]^{22}_D$ −45.4 (*c* 0.02, $CHCl_3$).

General Procedure for the Cross-Coupling Reaction. The palladium source [for $PdCl_2(PhCN)_2$, 0.1 or 0.2 mmol; for $Pd_2(dba)_3$·$CHCl_3$ and $Pd(PPh_3)_4$, 0.1 mmol; for $Pd_2(dba)_3$ and $AsPh_3$, 0.1 and 0.7 mmol, respectively] was added to a solution of corresponding haloallene (1 mmol) and stannane (1.5 mmol) in DMF (12 mL). At this point, the reaction mixture was thoroughly degassed using freeze−thaw cycles (3×) [where required, $(i\text{Pr})_2$NEt (1.5 mmol) was added at this point]. After stirring at 25 °C for the time period listed in Table 1, an aqueous saturated KF solution was added, the layers were separated, and the aqueous layer was extracted with EtOAc (3×). The combined organic layers were washed with brine (3×) and dried (Na_2SO_4), and the solvent was removed. The residue was purified by chromatography on silica gel to afford the corresponding vinylallene.

(+)-(1*R*,5*S*,2a*R*)- and (+)-(1*R*,5*S*,2a*S*)-5-(*tert*-Butyldimethylsilyloxy)-2-[(3*E*)-5-hydroxypenta-1,3-dienylidene]-1,3,3-trimethylcyclohexanol 9. Following the general procedure for the cross-coupling reaction, the reaction between bromoallene (a*R*)-**8a** (0.03 g, 0.08 mmol), stannane **7** (0.04 g, 0.16 mmol), and $Pd(PPh_3)_4$ (0.009 g, 0.008 mmol) afforded, after purification by chromatography on silica gel (70:30 hexane/EtOAc), 0.017 g (60%) of (1*R*,5*S*,2a*S*)-**9** and 0.008 g (28%) of (1*R*,5*S*,2a*R*)-**9**. Data for (1*R*,5*S*,2a*R*)-**9**: ^{1}H NMR (400 MHz, $CDCl_3$) δ 6.01 (ddt, J = 15.1, 10.2, 1.0 Hz, 1H), 5.88 (d, J = 10.2 Hz, 1H), 5.79 (dt, J = 15.2, 5.9 Hz, 1H), 4.25 (tt, J = 11.0, 4.2 Hz, 1H), 4.17 (dd, J = 5.9, 1.0 Hz, 2H), 2.10 (ddd, J = 13.1, 4.1, 2.2 Hz, 1H), 1.78 (ddd, J = 12.6, 4.1, 2.1 Hz, 1H), 1.59 (br s, 2H), 1.42 (dd, J = 13.1, 10.9 Hz, 1H), 1.33 (s, 3H), 1.31 (dd, J = 13.6, 10.4 Hz, 1H), 1.29 (s, 3H), 1.03 (s, 3H), 0.89 (s, 9H), 0.90 (s, 6H) ppm; ^{13}C NMR (100 MHz, $CDCl_3$) δ 203.5 (s), 129.6 (d), 127.6 (d), 116.4 (s), 96.3 (d), 72.8 (s), 64.8 (d), 63.4 (t), 49.7 (t), 49.1 (t), 35.5 (s), 32.1 (q), 31.2 (q), 29.2 (q), 25.9 (q, 3×), 18.2 (s), −4.6 (q, 2×) ppm; MS (ESI$^+$) 375 ([M + Na]$^+$, 100); HRMS (ESI$^+$) calcd for $C_{20}H_{36}NaO_3Si$, 375.2326; found, 375.2323; IR (NaCl) ν 3600−3100 (br, OH), 2956 (s, C−H), 2927 (s, C−H), 1939 (w, C═C═C); $[\alpha]^{22}_D$ +86.0 (*c* 0.02, MeOH). Data for (1*R*,5*S*,2a*S*)-**9**: ^{1}H NMR (400 MHz, $CDCl_3$) δ 6.07 (ddt, J = 14.8, 10.4, 1.0 Hz, 1H), 6.00 (d, J = 10.4 Hz, 1H), 5.80 (dt, J = 14.8, 5.8 Hz, 1H), 4.25 (tt, J = 11.1, 4.2 Hz, 1H), 4.18 (dd, J = 5.8, 1.0 Hz, 2H), 2.08 (ddd, J = 13.1, 4.2, 1.8 Hz, 1H), 1.75 (ddd, J = 12.6, 4.1, 2.1 Hz, 1H), 1.71−1.54 (br s, 1H), 1.38 (dd, J = 13.1, 10.9 Hz, 1H), 1.32 (s, 3H), 1.31 (s, 3H), 1.32−1.30 (m, 1H), 1.03 (s, 3H), 0.89 (s, 9H), 0.08 (s, 6H) ppm; ^{13}C NMR (100 MHz, $CDCl_3$) δ 203.2 (s), 129.9 (d), 127.8 (d), 116.4 (s), 96.6 (d), 72.9 (s), 64.8 (d), 63.3 (t), 49.5 (t), 48.9 (t), 35.3 (s), 32.0 (q), 31.2 (q), 29.9 (q), 25.9 (q, 3×), 18.1 (s), −4.6 (q, 2×) ppm; MS (ESI$^+$) 375 ([M + Na]$^+$, 100); HRMS (ESI$^+$) calcd for $C_{20}H_{36}NaO_3Si$, 375.2326; found, 375.2324; IR (NaCl) ν 3600−3100 (br, OH), 2956 (s, C−H), 2927 (s, C−H), 1939 (w, C═C═C); $[\alpha]^{22}_D$ +165.4 (*c* 0.02, MeOH).

(+)-(1*S*,3*R*,4a*R*)- and (+)-(1*S*,3*R*,4a*S*)-3-Hydroxy-4-[(*E*)-5-hydroxypenta-1,3-dienylidene]-3,5,5-trimethylcyclohexyl Acetate 10. Following the general procedure for the cross-coupling reaction, the reaction between iodoallene (a*R*)-**2b** (0.02 g, 0.06 mmol), stannane **7** (0.03 g, 0.08 mmol), and $PdCl_2(PhCN)_2$ (0.002 g, 0.006 mmol) afforded, after purification by chromatography on silica gel (60:40 hexane/EtOAc), 0.006 g (12%) of (1*S*,3*R*,4a*R*)-**10** and 0.008 (28%) of (1*S*,3*R*,4a*S*)-**10**. Data for (1*S*,3*R*,4a*R*)-**10**: ^{1}H NMR (400 MHz, $CDCl_3$) δ 6.03 (ddt, J = 15.1, 10.3, 1.3 Hz, 1H), 5.92 (d, J = 10.3 Hz, 1H), 5.80 (dt, J = 15.1, 5.8 Hz, 1H), 5.34 (tt, J = 11.5, 4.2 Hz, 1H), 4.18 (dd, J = 5.8, 1.0 Hz, 2H), 2.24 (ddd, J = 12.8, 4.2, 2.2 Hz, 1H), 2.03 (s, 3H), 1.94 (ddd, J = 12.5, 4.1, 2.2 Hz, 1H), 1.74 (s, 1H), 1.53 (s, 1H), 1.47 (dd, J = 12.7, 11.6 Hz, 1H), 1.38 (t, J = 12.0 Hz, 1H), 1.34 (s, 6H), 1.06 (s, 3H) ppm; ^{13}C NMR (100 MHz, $CDCl_3$) δ 203.5 (s), 170.5 (s), 129.9 (d), 127.2 (d), 115.8 (s), 96.6 (d), 72.4 (s), 68.0 (d), 63.3 (t), 45.2 (t), 45.0 (t), 35.5 (s), 32.0 (q), 31.0 (q), 29.1 (q), 21.4 (q) ppm; MS (ESI$^+$) 303 ([M + Na]$^+$, 100); HRMS (ESI$^+$) calcd for $C_{16}H_{24}NaO_4$, 303.1567; found, 303.1564; IR (NaCl) ν 3600−3100 (br, OH), 2963 (s, C−H), 2926 (s, C−H), 1939 (w, C═C═C); $[\alpha]^{22}_D$ +285.2 (*c* 0.02, MeOH). Data for (1*S*,3*R*,4a*S*)-**10**: ^{1}H NMR (400 MHz, $CDCl_3$) δ 6.09 (dd, J = 15.0, 10.4 Hz, 1H), 6.01 (d, J = 10.4 Hz, 1H), 5.80 (dt, J = 15.0, 5.6 Hz, 1H), 5.33 (tt, J = 11.5, 4.1 Hz, 1H), 4.18 (s, 2H), 2.21 (ddd, J = 12.8, 4.1, 2.1 Hz, 1H), 2.02 (s, 3H), 1.91 (ddd, J = 12.3, 4.0, 2.1 Hz, 1H), 1.44 (t, J = 12.0 Hz, 1H),

1.37 (s, 3H), 1.33 (s, 3H), 1.33 (t, J = 11.5 Hz, 1H), 1.05 (s, 3H) ppm; ^{13}C NMR (100 MHz, $CDCl_3$) δ 203.2 (s), 170.6 (s), 130.2 (d), 127.2 (d), 115.6 (s), 96.9 (d), 72.4 (s), 68.1 (d), 63.1 (t), 45.0 (t), 44.9 (t), 35.2 (s), 31.9 (q), 31.0 (q), 29.7 (q), 21.4 (q) ppm; MS (ESI$^+$) 303 ([M + Na]$^+$, 100); HRMS (ESI$^+$) calcd for $C_{16}H_{24}NaO_4$, 303.1567; found, 303.1567; IR (NaCl) ν 3600−3100 (br, OH), 2965 (s, C−H), 2926 (s, C−H), 1940 (w, C═C═C); $[\alpha]^{22}_D$ +256.8 (c 0.03, MeOH).

General Procedure for the Protection of Alcohols with TMSOTF. To a stirred solution of alcohol **2** (0.17 mmol) in CH_2Cl_2 (0.8 mL) at 0 °C were added 2,6-lutidine (2.05 mmol) and TMSOTf (1.37 mmol). The mixture was allowed to warm up to 25 °C (2 h), and the reaction was quenched with water and extracted with AcOEt (3×). The combined organic layers were washed with brine (3×) and dried (Na_2SO_4), and the solvent was removed. The residue was purified by chromatography on silica gel (97:1:2 hexane/AcOEt/Et_3N) to afford the corresponding protected alcohol.

(−)-(1*S*,3*R*,4a*R*)-4-(2-Iodovinylidene)-3,5,5-trimethyl-3-(trimethylsilyloxy)cyclohexyl Acetate 11b. Following the general procedure for the protection of alcohols as TMS ethers, the reaction between alcohol (a*R*)-**2b** (0.06 g, 0.17 mmol) and TMSOTf in the presence of 2,6-lutidine afforded, after purification by chromatography on silica gel (97:1:2 hexane/AcOEt/Et_3N), 0.054 g of a yellow oil (75%) identified as (1*S*,3*R*,4a*R*)-**11b**: ^{1}H NMR (400 MHz, acetone-d_6) δ 6.01 (s, 1H), 5.27 (tt, J = 11.6, 4.1 Hz, 1H), 2.21 (ddd, J = 12.6, 4.0, 2.4 Hz, 1H), 1.97 (s, 3H), 1.91 (ddd, J = 12.3, 4.2, 2.0 Hz, 1H), 1.47 (s, 3H), 1.39 (dd, J = 12.0, 11.6 Hz, 1H), 1.33 (t, J = 12.1 Hz, 1H), 1.33 (s, 3H), 1.14 (s, 3H), 0.13 (s, 9H) ppm; ^{13}C NMR (100 MHz, acetone-d_6) δ 203.6 (s), 171.3 (s), 120.1 (s), 75.8 (s), 68.8 (d), 48.6 (t), 46.6 (t), 39.9 (d), 36.7 (s), 32.6 (q), 31.1 (q), 30.8 (q), 22.2 (q), 3.3 (q, 3×) ppm; MS (FAB$^+$) 423 ([M + 1]$^+$, 25), 422 ([M]$^+$, 4); HRMS (FAB$^+$) calcd for $C_{16}H_{27}IO_3Si$, 422.0774; found, 422.0764; IR (NaCl) ν 2961 (s, C−H), 1950 (w, C═C═C), 1741 (s, C═O); $[\alpha]^{22}_D$ −49.1 (c 0.14, MeOH).

(+)-(1*S*,3*R*,4a*R*)-4-(2-Bromovinylidene)-3,5,5-trimethyl-3-(trimethylsilyloxy)cyclohexyl Acetate 11a. Following the general procedure for the protection with TMSOTF, the reaction between alcohol (a*R*)-**2a** (0.055 g, 0.16 mmol) and TMSOTf in the presence of 2,6-lutidine afforded, after purification by chromatography on silica gel (97:1:2 hexane/AcOEt/Et_3N), 0.057 g of a yellow oil (89%) identified as (1*S*,3*R*,4a*R*)-**11a**: ^{1}H NMR (400 MHz, acetone-d_6) δ 6.23 (s, 1H), 5.29 (tt, J = 11.5, 4.0 Hz, 1H), 2.24 (ddd, J = 12.7, 3.9, 2.4 Hz, 1H), 1.98 (s, 3H), 1.94 (ddd, J = 12.5, 4.2, 2.5 Hz, 1H), 1.48 (s, 3H), 1.43 (t, J = 12.0 Hz, 1H), 1.36 (t, J = 12.0 Hz, 1H), 1.35 (s, 3H), 1.14 (s, 3H), 0.14 (s, 9H) ppm; ^{13}C NMR (100 MHz, acetone-d_6) δ 200.1 (s), 171.2 (s), 125.1 (s), 76.0 (s), 75.8 (d), 68.7 (d), 48.7 (t), 46.7 (t), 37.4 (s), 32.8 (q), 31.0 (q), 30.4 (q), 22.2 (q), 3.3 (q, 3×) ppm; MS (FAB) m/z (%) 376 ([M]$^+$ [^{81}Br], 5), 374 ([M]$^+$ [^{79}Br], 5), 317 ([M − CO_2CH_3]$^+$ [^{81}Br], 30), 316 (21), 315 ([M − CO_2CH_3]$^+$ 33), 314 (16), 236 (19), 235 (82), 227 (52), 226 (16), 225 (52), 157 (18), 156 (100); HRMS calcd for $C_{16}H_{27}{}^{81}BrO_3Si$, 376.0892 and $C_{16}H_{27}{}^{79}BrO_3Si$, 374.0913; found, 376.0906 and 374.0922; IR (NaCl) ν 3057 (s, C−H), 1949 (w, C═C═C), 1742 (s, C═O); $[\alpha]^{22}_D$ +94.5 (c 0.03, MeOH).

(+)-(1*S*,3*R*,4a*R*)- and (−)-(1*S*,3*R*,4a*S*)-4-[(*E*)-5-Hydroxypenta-1,3-dienylidene]-3,5,5-trimethyl-3-(trimethylsilyloxy)cyclohexyl Acetate 12. Following the general procedure for Stille cross-coupling, the reaction between iodoallene (a*R*)-**11a** (0.015 g, 0.04 mmol), stannane **7** (0.020 g, 0.06 mmol), and $Pd_2dba_3\cdot CHCl_3$ (0.004 g, 0.004 mmol) afforded, after purification by chromatography on silica gel (80:20 hexane/EtOAc), 0.011 g (77%) of (1*S*,3*R*,4a*R*)-**12** and 0.003 (21%) of (1*S*,3*R*,4a*S*)-**12**. Data for (1*S*,3*R*,4a*R*)-**12**: ^{1}H NMR (400 MHz, acetone-d_6) δ 6.05 (ddt, J = 15.1, 10.3, 1.6 Hz, 1H), 5.94 (d, J = 10.3 Hz, 1H), 5.82 (dt, J = 15.1, 5.3 Hz 1H), 5.30 (tt, J = 11.6, 4.1 Hz, 1H), 4.10 (td, J = 5.5, 1.5 Hz, 2H), 3.74 (t, J = 5.6 Hz, 1H), 2.19 (ddd, J = 12.4, 4.1, 2.3 Hz, 1H), 1.96 (s, 3H), 1.91 (ddd, J = 12.3, 4.1, 2.3 Hz, 1H), 1.5−1.4 (m, 1H), 1.41 (s, 3H), 1.4−1.3 (m, 1H), 1.32 (s, 3H), 1.05 (s, 3H), 0.12 (m, 9H) ppm; ^{13}C NMR (100 MHz, acetone-d_6) δ 204.7 (s), 171.3 (s), 133.6 (d), 127.0 (d), 116.6 (s), 98.2 (d), 76.6 (s), 69.3 (d), 63.8 (t), 49.3 (t), 47.2 (t), 37.0 (s), 33.6 (q), 31.6 (q), 30.4 (q), 30.3 (q), 22.2 (s), 3.3 (q, 3×) ppm; MS (ESI$^+$) 375 ([M + Na]$^+$, 100); HRMS (ESI$^+$) calcd for $C_{19}H_{32}NaO_4Si$, 375.1962; found, 375.1958; IR (NaCl) ν 3600−3100 (br, OH), 2961 (s, C−H), 2866 (s, C−H), 1941 (w, C═C═C); $[\alpha]^{22}_D$ +42.4 (c 0.04, MeOH). Data for (1*S*,3*R*,4a*S*)-**12**: ^{1}H NMR (400 MHz, acetone-d_6) δ 6.2−6.1 (m, 1H), 6.08 (d, J = 10.5 Hz, 1H), 5.83 (dt, J = 14.6, 5.4 Hz, 1H), 5.30 (tt, J = 11.6, 4.2 Hz, 1H), 4.11 (td, J = 5.5, 1.4 Hz, 2H), 3.74 (t, J = 5.6 Hz, 1H), 2.17 (ddd, J = 12.4, 4.1, 2.3 Hz, 1H), 1.97 (s, 3H), 1.90 (ddd, J = 12.2, 4.2, 2.3 Hz, 1H), 1.42 (s, 3H), 1.4−1.3 (m, 1H), 1.37 (s, 3H), 1.29 (t, J = 11.9 Hz, 1H), 1.06 (s, 3H), 0.15 (s, 9H) ppm; ^{13}C NMR (100 MHz, acetone-d_6) δ 204.1 (s), 171.3 (s), 134.2 (d), 126.7 (d), 116.9 (s), 98.7 (d), 76.7 (s), 69.4 (d), 63.9 (t), 49.3 (t), 47.2 (t), 36.9 (s), 33.6 (q), 31.5 (q), 31.3 (q), 31.1 (q), 22.2 (s), 3.5 (q, 3×) ppm; MS (ESI$^+$) 375 ([M + Na]$^+$, 100); HRMS (ESI$^+$) calcd for $C_{19}H_{32}NaO_4Si$, 375.1962; found, 375.1958; IR (NaCl) ν 3600−3100 (br, OH), 2961 (s, C−H), 2866 (s, C−H), 1940 (w, C═C═C); $[\alpha]^{22}_D$ −43.0 (c 0.11, MeOH).

(+)-(5*E*,1*R*,4*S*,6*R*)-(4-(*tert*-Butyldimethylsilyloxy)-2,2,6-trimethyl-7-oxabicyclo[4.1.0]heptan-1-yl)pent-2-en-4-yn-1-ol 15. $Pd(PPh_3)_4$ (0.002 g, 0.002 mmol) and CuI (0.0003 g, 0.002 mmol) were added to a solution of alkyne **13**[6b] (0.049 g, 0.17 mmol) and iodide **14**[6b] (0.037 g, 0.20 mmol) in iPr_2NH (0.9 mL). After stirring for 1.5 h, a saturated aqueous solution of NH_4Cl was added and the mixture was extracted with Et_2O (3×). The combined organic layers were washed with brine (3×) and dried (Na_2SO_4), and the solvent was evaporated. The residue was purified by column chromatography (silica gel, 80:20 hexane/EtOAc) to afford 0.049 g (84%) of a yellow oil identified as **15**: ^{1}H NMR (400 MHz, $CDCl_3$) δ 6.24 (dt, J = 15.9, 5.1, 1H), 5.75 (d, J = 15.9, 1H), 4.17 (s, 2H), 3.8−3.7 (m, 1H), 2.20 (dd, J = 14.5, 4.9, 1H), 1.9−1.8 (m, 1H), 1.63 (dd, J = 14.5, 8.0, 1H), 1.5−1.4 (m, 1H), 1.44 (s, 3H), 1.20 (s, 3H), 1.2−1.1 (m, 1H), 1.07 (s, 3H), 0.83 (s, 9H), 0.00 (s, 6H) ppm; ^{13}C NMR (100 MHz, $CDCl_3$) δ 142.5 (d), 109.7 (d), 87.1 (s), 83.7 (s), 67.1 (s), 64.3 (d), 63.9 (s), 62.7 (t), 45.7 (t), 40.3 (t), 34.4 (s), 29.7 (q), 25.84 (q), 25.7 (q), 21.8 (q), 18.1 (s), −4.7 (q), −4.8 (q) ppm; MS (ESI$^+$) m/z (%) 389 (M$^+$ + 39, 13), 373 (M$^+$ + 23, 33), 351 (M$^+$ + 1, 100), 333 (7), 173 (7); HMRS (ESI$^+$) calcd for $C_{20}H_{35}O_3Si$, 351.2350; found, 351.2346; IR (NaCl) ν 3600−3100 (br, OH), 2954 (s, C−H), 2930 (s, C−H), 2858 (s, C−H), 2150 (w, C≡C); $[\alpha]^{19}_D$ + 39.4 (c 0.17, MeOH).

(1*R*,5*S*,2a*R*)-5-(*tert*-Butyldimethylsilyloxy)-2-[(3*E*)-5-hydroxypenta-1,3-dienylidene]-1,3,3-trimethylcyclohexanol 9. DIBAL-H (1.41 mL, 1 M in THF, 1.41 mmol) was added to a solution of **15** (0.049 g, 0.141 mmol) in CH_2Cl_2 (1.4 mL) at 0 °C, and the mixture was stirred for 2.5 h at 0 °C and for 1 h at 25 °C. After careful addition of H_2O (5 mL) at 0 °C and a 10% aqueous solution of HCl, the mixture was extracted with EtOAc (3×). The combined organic layers were washed with brine (3×), dried (Na_2SO_4), and concentrated. The residue was purified by column chromatography (silica gel, 70:30 hexane/EtOAc) to afford 0.025 g (50%) of a yellow oil identified as (1*R*,5*S*,2a*R*)-**9**.

Computational Details. All computations in this study have been performed using the Gaussian03 suite of programs.[17] To include electron correlation at a reasonable computational cost, density functional theory (DFT)[23] was used. The Becke three-parameter exchange functional and the nonlocal correlation functional of Lee, Yang, and Parr (B3LYP) was selected.[24] Given the complexity of the structures and transition states, the 6-31G* basis set for C, H, and P, in conjunction with the Stuttgart/Dresden -relativistic-effective core potentials for Pd and Br, was chosen to compute the geometries, energies, and normal mode vibration frequencies of the starting material, the corresponding transition structures, and the products. No symmetry constraints were imposed during

(23) (a) Parr, R. G.; Yang, W. *Density Functional Theory of Atoms and Molecules*; Oxford: New York, 1989. (b) Ziegler, T. *Chem. Rev.* **1991**, *91*, 651.
(24) Lee, C.; Yang, W.; Parr, R. G. *Phys. Rev. B* **1988**, *37*, 785.

structural optimizations. The stationary points were characterized by means of harmonic analysis, and for all the transition structures, the vibration related to the imaginary frequency was confirmed to correspond to the nuclear motion along the reaction coordinate under study. All energy results presented correspond to Gibbs energies at 298.15 K. The effect of the solvent at 298.15 K was taken into account through single-point calculations at each optimized geometry using the COSMO model[18] as implemented in Gaussian03.

Acknowledgment. The authors are grateful to the European Union (EPITRON, LSHC-CT-2005-518417), the Xunta de Galicia (Parga Pondal Contract to M.P.; PGIDIT07PXIBIB3174174 PR to R.A.), and the Spanish Ministerio de Educación y Ciencia (SAF07-63880-FEDER).

Supporting Information Available: General experimental methods, physical and spectroscopic data for all compounds, and final SCF energies, geometries, and number of imaginary frequencies. This material is available free of charge via the Internet at http://pubs.acs.org.

JO800756B